

Adsorption of Paracetamol Using Activated Carbon of Dende and Babassu Coconut Mesocarp

R. C. Ferreira, H. H. C. De Lima, A. A. Cândido, O. M. Couto Junior, P. A. Arroyo, K. Q De Carvalho, G. F. Gauze, M. A. S. D. Barros

Abstract—Removal of the widespread used drug paracetamol from water was investigated using activated carbon originated from dende coconut mesocarp and babassu coconut mesocarp. Kinetic and equilibrium data were obtained at different values of pH. Both activated carbons showed high efficiency when $\text{pH} \leq \text{pH}_{\text{PZC}}$ as the carbonil group of paracetamol molecule are adsorbed due to positively charged carbon surface. Microporosity also played an important role in such process. Pseudo-second order model was better adjusted to the kinetic results. Equilibrium data may be represented by Langmuir equation.

Keywords—Adsorption, activated carbon, babassu, dende.

I. INTRODUCTION

THE production of pharmaceuticals has increased rapidly during the last decades as they are used for the health of humans and animals. After their use, large amount of pharmaceuticals are discharged into the water environment, and they have been detected in wastewater and surface water at ng/L to µg/L levels [1], [2]. It has been demonstrated that conventional wastewater treatments are not effective to eliminate or at least degrade most of these compounds. Therefore, residual quantities remain in treated water and have been accumulating in drinking water [3], [4].

As water is an essential resource for life in all ecosystems, a great effort has been made in the past decades to improve the water treatment. One of the technologies is adsorption. Among the most promising biosorbent materials for aquatic environments the use of black tea residue [5], sawdust [6], sugar cane bagasse [7], cork powder, peach stones [8], eggshell waste [9], olive stones [10], aquatic plants [11], mango peel [12], coconut mesocarp [13], banana peel [14], bamboo stem and coconut shells [15], stand out. Nevertheless, activated carbons are always one of the best choices, as they involve a well-established and effective technology widely used. Their adsorption properties are due the large accessible

surface area and pore volume as well as possibility of regeneration [8], [16], [17]. Activated carbons may be obtained from a large number of residues of vegetal species. The ones related to native species aggregate advantages related to feasibility and low costs as well. Particularly, babassu and dende are Brazilian palm trees that produce vegetal oil. After extraction, the shells are burned to obtain the activated carbon. Their efficiency in the adsorption of medicines presented in wastewater has been already reported [18]. Then, the objective of this paper was to study the activated carbon of dende coconut mesocarp and babassu coconut mesocarp in the adsorption of paracetamol. Kinetic and equilibrium data were obtained at different values of pH.

II. MATERIALS AND METHODS

A. Materials

The activated carbon of dende coconut mesocarp (DD) was provided by the Bahiacarbon Agro Ind. (Bahia, Brazil) whereas babassu coconut mesocarp (BB) was donated by Tobasa Agro Ind. (Tocantins, Brazil). The samples were previously washed, dried for 24 h at 60°C and sieved. Particles with average diameter of 0.180 mm (70-100 mesh) were selected for the adsorption experiments.

Nanotexture of the carbon materials was characterized by N_2 adsorption at 196 and 0°C, respectively, in conventional volumetric apparatus (ASAP 2000, from Micromeritics). Before the experiments, the samples were outgassed under vacuum at 300°C. The isotherms were used to calculate the specific surface area (S_{BET}), total pore volume, V_{TOTAL} , and pore size distribution. The S_{BET} was assessed applying the BET equation (in the range $0.05 < p/p_0 < 0.15$). The microporous volume ($V_{\alpha_{\text{total}}} - 6 \text{ \AA} < \text{pore diameter} < 20 \text{ \AA}$) and ultramicroporous volume ($V_{\alpha_{\text{Ultra}}} - \text{related to pores} < 6 \text{ \AA}$) were calculated using the α_s method [19]. The total pore volume was determined by the quantity adsorbed at $p/p_0 = 0.95$. The $V_{\alpha_{\text{Total}}}$ (microporous total volume) and $V_{\alpha_{\text{Ultra}}}$ (ultramicroporous volume) were calculated using the method of the demanding [19]. The volume of supermicropores ($V_{\alpha_{\text{Super}}}$) was obtained by the difference: $V_{\alpha_{\text{Total}}} - V_{\alpha_{\text{Ultra}}}$. The mesoporous volume (V_{Meso}) was calculated by $V_{\text{TOTAL}} - V_{\alpha_{\text{Total}}}$ difference.

The pH of the point of zero charge (pH_{PZC}) was also estimated in both adsorbents using the mass titration procedure [20].

Paracetamol (acetaminophen or N-acetyl-p-aminophenol) molecule is shown in Fig. 1. Paracetamol powder was added

R. C. Ferreira, H. H. C. de Lima, P. A. Arroyo, and M.A.S.D. Barros are with the Chemical Engineering Department, State University of Maringá, Maringá-PR, Brazil. (phone: +55 44 9922 1101; e-mail: angelicabarros.deq@gmail.com)

O. M. Couto Junior was with the Chemical engineering Department, State University of Maringá and now is with the Engineering Department, University Center of Maringá.

A. A. Cândido and G. F. Gauze are with the Chemistry Department, State University of Maringá, Maringá-PR, Brazil (e-mail: giselegauze@yahoo.com.br)

K. Q de Carvalho is with the Academic Department of Civil Construction, Federal Technological University of Paraná, Curitiba-PR, Brazil (e-mail: regiane.cristina.1989@gmail.com)

to 10% (v/v) of methanol (Anidrol) diluted in Milli-Q water in order to obtain 50 mg.dm⁻³. pH of paracetamol solutions were corrected to pH 2, pH p_{H_{PZC}} of DD and BB samples as well as pH 11 using NaOH or HCl 0.1 mol dm⁻³ solutions.

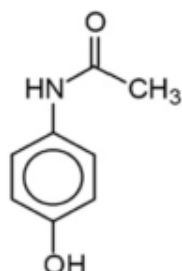


Fig. 1 Molecular structure of paracetamol

Gaussian 09 program package [21] modeled the electronic structure of the paracetamol in the preferred conformation in pH 2 and pH 11. Surfaces of potential energy were calculated through the semi-empirical method PM6 in order to determine the structure in space. The lowest energy structures were then optimized in a high level of theory B3LYP/6-311+G(d,p) and the map of electrostatic potential surface of the optimized structures generated.

B. Kinetic Adsorption of Paracetamol

Adsorption kinetics should be investigated in order to determine the equilibrium time and to elucidate the mechanism of the adsorption process [16].

The kinetic and equilibrium data were obtained in three different pH solutions and at the constant temperature of 25°C.

Kinetic experiments were carried out adding 10 mg of DD or BB in 20 cm³. The system was stirred at 150 rpm. Samples at different running times (from 5 minutes up to 8 hours) were collected. After filtration, the amount of paracetamol was determined by spectrophotometer DR 5000 in 240 nm. The amount of adsorbed paracetamol was calculated according to the mass balance:

$$q_t = \frac{(C_0 - C_t)V}{W} \quad (1)$$

where q_t is the amount (mg g⁻¹) of paracetamol adsorbed at time t , C_0 is the paracetamol initial concentration (50 mg dm⁻³), C_t is the paracetamol concentration at time t (mg dm⁻³), V is the volume of the adsorbate solution and W is the weight (g) of dried activated carbon of dende coconut mesocarp.

Models of pseudo-first order [22] and pseudo-second order [23] were adjusted to the experimental data.

The pseudo first-order rate equation of Lagergren based on solid capacity is expressed as:

$$\frac{dq_t}{dt} = k_1(q_e - q_t) \quad (2)$$

Integration (2) for the initial conditions $t = 0$ and $q_t = 0$ originates the pseudo-first order rate equation:

$$q_t = q_e(1 - e^{-k_1 t}) \quad (3)$$

The pseudo-second order kinetic model equation is expressed as:

$$\frac{dq_t}{dt} = k_2(q_e - q_t)^2 \quad (4)$$

Integration (4) for the initial conditions $t = 0$ and $q_t = 0$ gives the pseudo-second order rate equation as:

$$q_t = \frac{q_e^2 k_2 t}{1 + k_2 q_e t} \quad (5)$$

C. Equilibrium Data

Equilibrium adsorption studies were carried out adding different amount of adsorbent (0.07-60 mg) to 20 cm³. After reaching equilibrium, the solution was filtered and concentration of paracetamol in the solid phase (q_e) was obtained through (1). In this case t refers to the equilibrium time, which was obtained in the kinetic experiments.

In this study Langmuir and Freundlich isotherm models were fitted to the equilibrium data.

The Langmuir adsorption isotherm equation, expressed as follows requires for its applicability a mono-layered coverage on the surface of adsorbent [24]:

$$q_e = \frac{q_{\max} k_L C_e}{1 + k_L C_e} \quad (6)$$

where k_L is the Langmuir constant related to the adsorption energy (L mg⁻¹), q_{\max} is the maximum amount of paracetamol retained in the solid phase and C_e (mg L⁻¹) stands for paracetamol concentration in the fluid phase that is in equilibrium with q_e .

The empirical Freundlich isotherm is expressed by [25]:

$$q_e = k_F C_e^{1/n} \quad (7)$$

where k_F and n are the Freundlich constants.

The Freundlich equation was successfully used to fit the experimental data for many fluid-solid systems, but one of the main drawbacks of this equation is that it doesn't tend to a limiting value whereas the equilibrium concentration increases. Generally, Freundlich equation is used to model multilayer adsorption.

III. RESULTS AND DISCUSSION

A. Characterization of the Adsorbent

The nitrogen adsorption-desorption isotherms are presented in Fig. 2. DD and BB were typical microporous-mesoporous adsorbents (type I in the IUPAC classification) with a hysteresis loop (H4 types) in the desorption branch at relative pressures above 0.5. The adsorption-desorption hysteresis on activated carbon isotherm showed clearly that liquid nitrogen was condensed in slit-shaped mesopores [26].

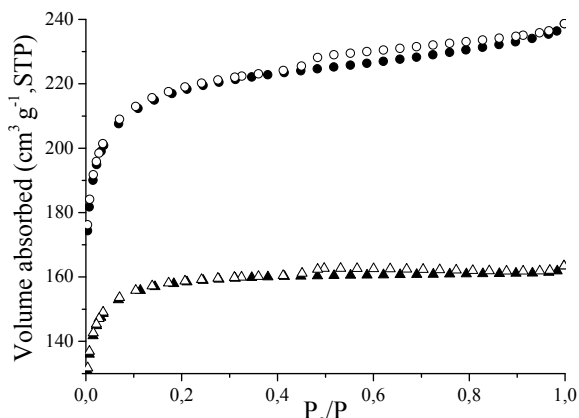


Fig. 2. N₂ adsorption-desorption isotherms at 77 K of DD (●) adsorption and (○) desorption and BB; (▲) adsorption and (Δ) desorption

For low relative pressure a sharp knee is observed followed by an almost horizontal plateau over a wide range of high relative pressures. This shape is related to a predominant microporous structure.

Fig. 3 depicts the pore size distribution. In agreement with the N₂ isotherm shape, DD and BB had a huge contribution of micropores although some mesoporosity was also presented, mainly in the DD sample, where a pronounced pick close to 40 Å was observed. Actually, the average pore diameter was estimated as 34.5 Å for DD whereas BB had an average pore diameter of 11.5 Å.

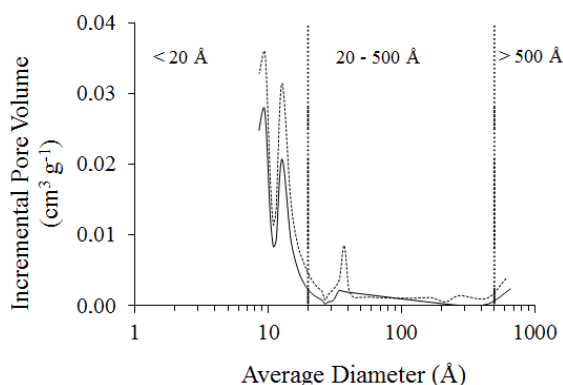


Fig. 3 Pore size distribution: (···) dende carbon; (—) babassu carbon

TABLE I

NANOTEXTURAL CHARACTERISTICS OF THE CABONS BABASSU AND DENDÉ

Sample	A _{BET}	V _{TOTAL}	V _{MESO}	α _s method			pH _{PZC}
				V _{aTOTAL}	V _{aULTRA}	V _{aSUPER}	
DD	672	0.37	0.08	0.29	0.20	0.09	6.5
BB	484	0.35	0.03	0.22	0.16	0.06	3.9

$$A_{BET} = m^2 g^{-1}; V_{TOTAL}, V_{MESO}, V_{aTOTAL}, V_{aULTRA}, V_{aSUPER} = cm^3 g^{-1}$$

As shown in Table I, DD had higher specific surface area (672 m² g⁻¹). However, micropores contributed to 78% of the total volume of pores, less than the 88% seen in the BB sample. Probably it was a consequence of the pick near 40 Å already discussed.

It was also noteworthy that, according to pH_{PZC}, BB had a more acid behavior probably due to acid superficial groups. Nevertheless, DD had almost a neutral surface. Such differences may be significant when investigating the adsorption mechanism.

B. Preferred Conformation of Paracetamol

Paracetamol is a weak acid with pK_a values between 9.0 and 9.50 [27]. At this pH half of molecules is in the neutral form whereas the other 50% is in the anionic form. Therefore, solutions with 2.0 < pH < 9.0 present neutral paracetamol molecules. In solutions with pH > 10 the anionic form predominates.

Fig. 4 shows the optimized structure and the electrostatic potential maps for both forms: neutral (a) obtained at pH 2 and anionic (b) at pH 11.

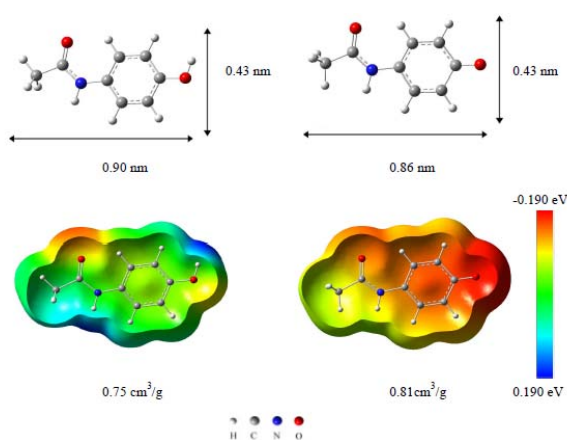


Fig. 4 Optimized structure and potential electrostatic map for the a) neutral (pH 2) and b) anionic (pH 11) forms of paracetamol

It can be seen that at pH 2 the paracetamol molecule is neutral with low electronic density. Actually, a significant electronic density can be attributed only to the carbonil group. At pH 11 the most important and clearly more pronounced region of high electronic density is located in the phenolic group, due to the acid dissociation.

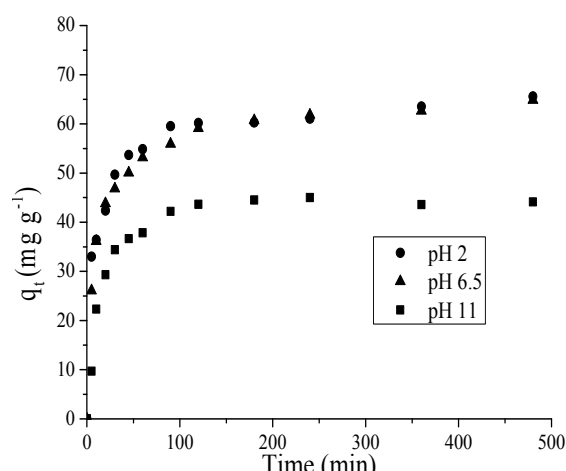
C. Kinetic Studies of Paracetamol

Results with acid paracetamol solution with pH 2, pH pH_{PZC} and basic solution with pH 11 is seen in Fig. 5 for DD and BB samples.

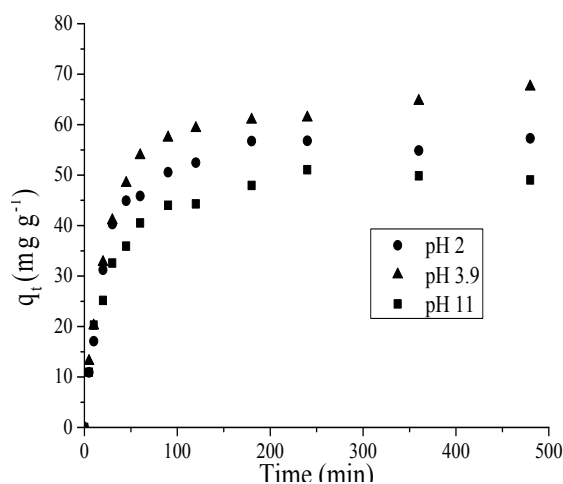
According to the kinetic results it can be seen that the system reached equilibrium in 240 minutes. Moreover, a rapid initial adsorption occurred due to a large number of surface sites available for adsorption.

According to Fig. 5, it can be also observed that in both systems, the acid solution (pH 2) and solution in the pH_{PZC} promoted significant removal of paracetamol. Possibly the positively charged surface of the adsorbent may attract the highest electronic charges of the neutral paracetamol molecule located in the C=O group. Then, chemisorption may have some contribution. As already discussed, under these conditions paracetamol was predominantly in its molecular

form (the anionic form accounts for less than 0.1 mol%) whereas the carbon surface sites are positively charged ($pH_{PZC} > \text{solution pH}$).



(a)



(b)

Fig. 5 Kinetic results of paracetamol adsorption at 25°C with different values of pH (a) dende carbon (b) babassu carbon

When adsorption occurs in the zero point charge, the carbon surface is neutral and the paracetamol charges may be weakly attracted to some superficial groups although physisorption seems to have a huge contribution due to the high microporosity of the activated carbons. On the other hand, in basic solutions, the paracetamol molecules have much higher density charge that was repelled by the negatively charges of the solid sample. In such case, physisorption may be more significant.

This phenomenon can be verified in Table II where the maximum amount of paracetamol experimentally retained in equilibrium is shown. At pH 2 the maximum removal in DD samples occurred. Nevertheless, paracetamol removal suffered a slightly decrease when DD was in contact with solution in

the zero point charge of 6.5. In such case the carbonil groups may induce some chemisorption although physisorption should have the greatest contribution, mainly in the micropores, where the molecule may be better retained, as already discussed. In basic solutions where $pH > pK_a$, the amount retained suffered a drastically decrease due to the anionic charges involved.

TABLE II
MAXIMUM AMOUNT OF PARACETAMOL ADSORBED IN EQUILIBRIUM
OBTAINED IN KINETIC RUNS

Activated carbon	q_t		
	pH 2	pH PCZ	pH 11
DD	65.57	64.85	44.12
BB	57.29	67.51	49.03

$q_t = \text{mg g}^{-1}$

BB samples showed the highest retention at the zero point charge. As the physisorption dominated due to the neutrality of the solid phase, microporosity provided higher adsorption [28]. In fact, adsorption of pharmaceutical compounds onto activated carbon has revealed that the amount of pollutant adsorbed is usually directly proportional to the micropore volume [8], [17], [29].

In Table III results of kinetic modeling are seen.

TABLE III
PARACETAMOL KINETIC FITTINGS

Sample	Kinetic model		pH		
			2	PZC	11
DD	Pseudo-first order	q _{eq}	59.11±1.892	58.31±1.756	43.07±0.797
		k ₁	0.092±0.016	0.081±0.013	0.055±0.005
		R ²	0.911	0.928	0.979
	Pseudo-Second order	q _{eq}	63.11±1.244	62.91±0.929	46.81±0.804
		k ₂	0.002±3.3x10 ⁻⁴	0.002±1.9x10 ⁻⁴	0.002±1.7x10 ⁻⁴
		R ²	0.976	0.988	0.978
BB	Pseudo-first order	q _{eq}	54.91±0.878	62.37±1.004	47.69±1.142
		k ₁	0.039±0.003	0.036±0.002	0.037±0.004
		R ²	0.988	0.988	0.972
	Pseudo-Second order	q _{eq}	60.73±1.175	69.31±0.888	52.53±0.756
		k ₂	8.7x10 ⁻⁴ ±9.0x10 ⁻⁵	6.8x10 ⁻⁴ ±4.6x10 ⁻⁵	0.001±7.8x10 ⁻⁵
		R ²	0.988	0.995	0.993

$q_{eq} = \text{mg g}^{-1}$; $k_1 = \text{h}^{-1}$

In both cases the pseudo-second order equation seemed to represent the experimental data as it showed higher R^2 and close to one. Moreover, parameters presented low deviation and the amount retained in equilibrium was similar to the experimental ones presented in Table II. Such model has been successfully applied to the adsorption of organic molecules such as dyes, herbicides, oils, and organic substances from aqueous solutions [30]. In all values of pH studied herein differences could be seen as a consequence of the small electrostatic attraction in acid solutions or electrostatic repulsion in basic solutions. This is in agreement with the fact that in pseudo-second order kinetics, chemisorption involves valence forces [30]. In fact, adsorption of organic molecules

from dilute aqueous solutions on carbon materials is a complex interplay between electrostatic and non-electrostatic interactions and that both interactions depend on the characteristics of the adsorbent and adsorbate, as well as the solution chemical properties [31].

D. Adsorption Isotherms

Fig. 6 illustrates the paracetamol adsorption isotherms on the studied carbons and Langmuir model that originated the best fit.

The activated carbon was classified as type L [32], showing a steep initial rise and a concave curvature at low equilibrium concentrations followed by a plateau or saturation limit. This is characteristic of systems where the adsorbate presented high affinity towards the adsorbent, and therefore indicated that no strong competition of the solvent took place for the active sites of adsorption. Acid pH provided again more concavely upward curvature indicating higher adsorption energy, which was in agreement with the electrostatic interaction of the carbonil group with the positively charged surface already explained.

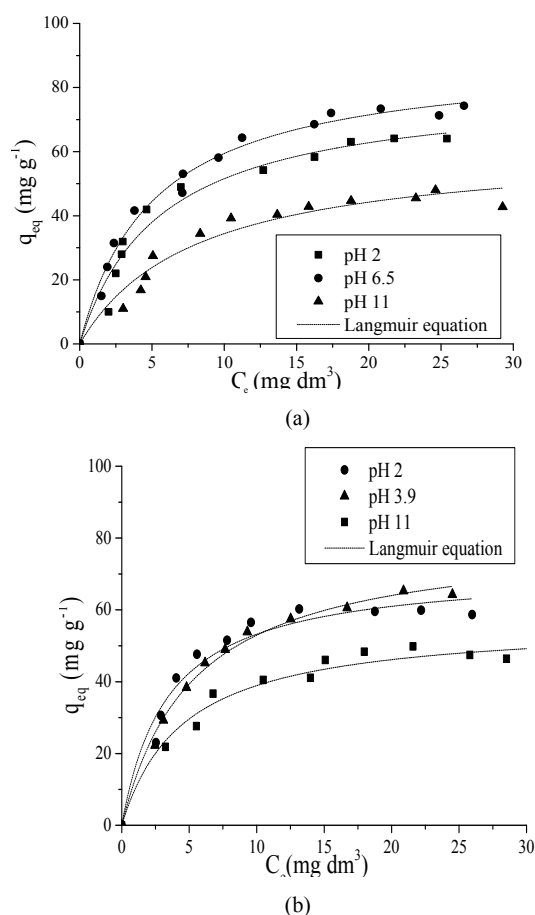


Fig. 6 Experimental adsorption isotherms of paracetamol with different values of pH (a) dende carbon (b) babassu carbon fitted by the Langmuir model

Table IV presents the maximum experimental retention of

both activated carbon whereas Table V shows the quantitative values of Freundlich and Langmuir adjustments. It may be seen that Langmuir adjustment originated the best fit with higher R^2 and low parameter deviation. Comparing values shown in Table IV and the q_{\max} from Langmuir, it may be seen that the estimated maximum amount was not experimentally reached. Then, only values of k_L should be discussed. As expected values of Table IV are similar do the ones shown in Table II obtained when kinetic data reached equilibrium.

TABLE IV
EXPERIMENTAL VALUES OF Q_{\max}

Activated carbon	$Q_{\max}(\text{exp})$		
	pH 2	pH PCZ	pH 11
DD	64.75	74.31	42.75
BB	58.91	65.29	45.94

$$Q_{\max}(\text{exp}) = \text{mg g}^{-1}$$

In all cases k_L for BB samples were higher than the ones obtained for DD. Such results were already expected since BB was more acid, with high amount of acid groups in the surface, than DD. Moreover, BB had higher contribution of micropores, where paracetamol may be better accommodated. It must be also emphasized such results are a consequence of the electrostatic attraction of the carbonil group.

IV. CONCLUSION

The potentialities of low-cost high-value activated carbons, obtained from dende and babassu coconut mesocarp for the removal of a widespread used drug (paracetamol) was investigated. Results show that the two activated carbons are suitable for paracetamol removal. Microporosity and mainly solutions with $\text{pH} \leq \text{pH}_{\text{PZC}}$ are of quite importance. Paracetamol easily diffuses into micropores and acid solutions promote paracetamol removal due to the attraction of the carbonil group to the positively charged carbon surface. Pseudo-second order model and Langmuir equation may represent the kinetic and equilibrium data, respectively.

TABLE V
LANGMUIR AND FREUNDLICH ADJUSTMENTS

LANGMUIR AND FREUNDLICH ADJUSTMENTS					
Sample	Isot. model		2	pH PZC	11
DD	Lang.	q _{max}	70.62±1.599	90.813±3.073	62.911±5.875
		k _L	0.280±0.026	0.187±0.019	0.117±0.029
		R ²	0.980	0.984	0.925
	Freund.	k _F	25.843±1.937	21.398±2.209	12.212±2.388
		1/n	0.281±0.349	0.404±0.235	0.422±0.393
		R ²	0.948	0.944	0.879
BB	Lang.	q _{max}	71.39±3.568	80.87±2.268	56.67±2.492
		k _L	0.293±0.052	0.189±0.016	0.218±0.018
		R ²	0.961	0.992	0.967
	Freund.	k _F	26.42±3.589	21.46±2.213	19.62±2.688
		1/n	0.278±0.689	0.369±0.297	0.279±0.615
		R ²	0.899	0.957	0.929

$$q_{\max} = \text{mg g}^{-1}; k_L = \text{L g}^{-1}$$

ACKNOWLEDGMENT

The authors thank the financial support of CAPES – Coordination of Superior Level Staff Improvement.

REFERENCES

- [1] Jelic A, Gros M, Ginebreda A, Cespedes-Sánchez R, Ventura F, Petrovic M, et al. Occurrence, partition and removal of pharmaceuticals in sewage water and sludge during wastewater treatment. *Water Res* 2011; 45:1165–76.
- [2] Verlicchi P, Al Aukidy M, Zambello E. Occurrence of pharmaceutical compounds in urban wastewater: removal, mass load and environmental risk after a secondary treatment--a review. *Sci Total Environ* 2012; 429:123–55.
- [3] Radjenović J, Petrović M, Barceló D. Fate and distribution of pharmaceuticals in wastewater and sewage sludge of the conventional activated sludge (CAS) and advanced membrane bioreactor (MBR) treatment. *Water Res* 2009; 43:831–41.
- [4] Rivera-Utrilla J, Sánchez-Polo M, Ferro-García MÁ, Prados-Joya G, Ocampo-Pérez R. Pharmaceuticals as emerging contaminants and their removal from water. A review. *Chemosphere* 2013; 93:1268–87.
- [5] Abdallah MAM. The potential of different bio adsorbents for removing phenol from its aqueous solution. *Environ Monit Assess* 2013;185:495–503.
- [6] Stankovic V, Bozic D, Gorgievski M, Bogdanovic G. Heavy metal ions adsorption from mine waters by sawdust. *Chem Ind Chem Eng Q* 2009; 15:237–49.
- [7] Soliman EM, Ahmed S a., Fadl A a. Removal of calcium ions from aqueous solutions by sugar cane bagasse modified with carboxylic acids using microwave-assisted solvent-free synthesis. *Desalination* 2011; 278:18–25.
- [8] Cabrita I, Ruiz B, Mestre a. S, Fonseca IM, Carvalho a. P, Ania CO. Removal of an analgesic using activated carbons prepared from urban and industrial residues. *Chem Eng J* 2010; 163:249–55.
- [9] Daraei H, Mittal A, Noorisepehr M, Daraei F. Kinetic and equilibrium studies of adsorptive removal of phenol onto eggshell waste. *Environ Sci Pollut Res Int* 2013; 20:4603–11.
- [10] Kütahyalı C, Eral M. Sorption studies of uranium and thorium on activated carbon prepared from olive stones: Kinetic and thermodynamic aspects. *J Nucl Mater* 2010; 396:251–6.
- [11] Baral SS, Das N, Roy Chaudhury G, Das SN. A preliminary study on the adsorptive removal of Cr(VI) using seaweed, *Hydrilla verticillata*. *J Hazard Mater* 2009; 171:358–69.
- [12] Foo KY, Hameed BH. Factors affecting the carbon yield and adsorption capability of the mangosteen peel activated carbon prepared by microwave assisted K₂CO₃ activation. *Chem Eng J* 2012;180:66–74.
- [13] Vieira AP, Santana SAA, Bezerra CWB, Silva HAS, Chaves JAP, de Melo JCP, et al. Kinetics and thermodynamics of textile dye adsorption from aqueous solutions using babassu coconut mesocarp. *J Hazard Mater* 2009; 166:1272–8.
- [14] Hossain MA, Ngo HH, Guo WS, Nguyen T V. Biosorption of Cu (II) From Water by Banana Peel Based Biosorbent : Experiments and Models of Adsorption and Desorption. *J Water Sustain* 2012; 2:87–104.
- [15] Khalil HPSA, Jawaid M, Firoozian P, Rashid U, Islam A, Akil HM. Activated Carbon from Various Agricultural Wastes by Chemical Activation with KOH: Preparation and Characterization. *J Biobased Mater Bioenergy* 2013; 7:708–14.
- [16] Mestre AS, Pires J, Nogueira JMF, Parra JB, Carvalho AP, Ania CO. Waste-derived activated carbons for removal of ibuprofen from solution: role of surface chemistry and pore structure. *Bioresour Technol* 2009; 100:1720–6.
- [17] Ruiz B, Cabrita I, Mestre a. S, Parra JB, Pires J, Carvalho a. P, et al. Surface heterogeneity effects of activated carbons on the kinetics of paracetamol removal from aqueous solution. *Appl Surf Sci* 2010; 256:5171–5.
- [18] Couto Jr. OM, Matos I, Fonseca IM da, Arroyo PA, Silva EA da, Barros MASD de. Effect of Solution pH and Influence of Water Hardness on Caffeine Adsorption onto Activated Carbons. *Can J Chem Eng* 2015; 93:68–77.
- [19] Rodriguez-reinoso F, Martin-martinez JM, Prado-burguete C, Mcenaney B. Standard Adsorption Isotherm for the Characterization of Activated Carbons. *J Phys Chem* 1987; 91:515–6.
- [20] Park J, Regalbuto JR. A simple, accurate determination of oxide PZC and the strong buffering effect of oxide surfaces at incipient wetness. *J Colloid Interface Sci* 1995; 175:239–52.
- [21] Frisch M, Trucks G, Schlegel H. Gaussian, Inc. Gaussian, Inc, Wallingford, ... 2010.
- [22] Lagergren S. Zur Theorie der sogenannten Adsorption gelöster Stoffe. *K Sven Vetenskapsakademiens, Handl* 1898;24:1–39.
- [23] Ho Y., McKay G. Pseudo-second order model for sorption processes. *Process Biochem* 1999; 34:451–65.
- [24] Langmuir I. The constitution and fundamental properties of solids and liquids. *J Am Chem Soc* 1916; 38:2221–95.
- [25] Ruthven DM. Principles of Adsorption and Adsorption Processes. John Wiley. 1984.
- [26] Guedidi H, Reinert L, Lévêque J-M, Soneda Y, Bellakhal N, Duclaux L. The effects of the surface oxidation of activated carbon, the solution pH and the temperature on adsorption of ibuprofen. *Carbon N Y* 2013;54:432–43.
- [27] Florey K. Analytical Profiles of Drug Substances. Vol. 3, vol. 3. Academic P, New York and London: 1974, p. 1–109.
- [28] Dubinin M.M. Adsorption in micropores. *J Colloid Interface Sci* 1967; 23:487–99.
- [29] Galhetas M, Mestre AS, Pinto ML, Gulyurtlu I, Lopes H, Carvalho AP. Carbon-based materials prepared from pine gasification residues for acetaminophen adsorption. *Chem Eng J* 2014;240:344–51.
- [30] Ho Y-S. Review of second-order models for adsorption systems. *J Hazard Mater* 2006; 136:681–9. doi:10.1016/j.jhazmat.2005.12.043.
- [31] Moreno-Castilla C. Adsorption of organic molecules from aqueous solutions on carbon materials. *Carbon N Y* 2004;42:83–94.
- [32] Giles CH, Macewan TH, Nakhwa SN, Smith D. Studies in Adsorption. Part XI.* A System of Classification of Solution Adsorption Isotherms, and its Use in Diagnosis of Adsorption Mechanisms and in Measurement of Specific Surface Areas of Solids. *J Chem Soc* 1960: 3973–93.